

Nonlinear propagation and continuum generation in microstructured optical fibers

Alexander L. Gaeta

School of Applied and Engineering Physics, Cornell University, Ithaca, New York 14853

Received December 5, 2001

A theoretical investigation of the propagation of femtosecond pulses under conditions similar to those of recent experiments in which a white-light continuum was generated in a microstructured fiber is presented. It is found that higher-order dispersion primarily determines the shape and width of the generated spectrum and that the fine spectral substructure exhibits extreme sensitivity to the initial pulse energy. © 2002 Optical Society of America

OCIS codes: 320.7140, 320.7110, 060.5530.

Propagation of ultrashort pulses in optical fibers near the zero-dispersion wavelength allows for relatively long interaction lengths with high peak intensities, which can result in dramatic nonlinear effects. This idea is perhaps best illustrated by recent experiments¹ in which pulses from a femtosecond Ti:sapphire laser were injected into a microstructured fiber with the zero-dispersion wavelength shifted far to the blue side (~800 nm) of that (1280 nm) of bulk fused silica. For input pulses with nanojoule energies, an extremely broad spectral continuum spanning from 400 to 1600 nm is generated at the output of the fiber. Such a coherent white-light source has been applied to ultrahigh-resolution imaging via optical coherence tomography² and has led to a revolution in the field of frequency metrology.^{3,4}

Microstructure fibers with small core sizes have been ideal for this nonlinear interaction, since the tight mode confinement that shifts the zero-dispersion point below 800 nm also enhances the effective nonlinearity of the propagating mode. Similarly, tapered fibers have also been used⁵ successfully to produce white-light continua. There have been numerous experimental and theoretical investigations⁶⁻⁹ of nonlinear propagation near the zero group-velocity dispersion point; however, in none of these studies did the interaction correspond to the highly nonlinear operating conditions of these recent experiments.

In this Letter a theoretical investigation of the nonlinear propagation of femtosecond pulses tuned near the zero-dispersion point of a fiber waveguide is presented. It is found that the spectral envelope of the generated continuum is determined primarily by the higher-order dispersion of the fiber. Specifically, the interplay between third-order dispersion (TOD) and self-phase modulation is found to dominate the propagation dynamics and largely determines the extent of the blue edge of the spectrum and the relative lack of broadening to the red edge. In addition, the spectrum exhibits a highly complicated substructure that is extremely sensitive to input pulse energy. These predictions were recently confirmed via single-pulse measurements by Gu *et al.*¹⁰

Pulse propagation is modeled inside the fiber by use of the one-dimensional nonlinear envelope equation^{11,12}

with inclusion of the effects of stimulated Raman scattering. It is assumed that the pulse propagates along the z axis with a wave-vector amplitude $k_0 = n_0\omega_0/c$, where n_0 is the linear refractive index of the material and ω_0 is the central frequency of the pulse. For an input pulse that is Gaussian in time such that the amplitude $A(z=0, t) = A_0 \exp(-t^2/2\tau_p^2)$, the equation for the normalized amplitude, $u(z, t) = A(z, t)/A_0$, can be expressed as

$$\frac{\partial u}{\partial \xi} = -i \sum_{n=2} \frac{L_{ds}}{n! L_{ds}^{(n)}} \frac{\partial^n u}{\partial \tau^n} + i \left(1 + \frac{i}{\omega_0 \tau_p} \frac{\partial}{\partial \tau} \right) p^{nl}, \quad (1)$$

where $L_{ds}^{(n)} = \tau_p^n / \beta_n$ is the n th-order dispersion length, β_n ($n \geq 2$) is the n th-order dispersion constant,¹³ $L_{ds} = |L_{ds}^{(2)}|$ is the dispersion length, $\xi = z/L_{ds}$ is the normalized distance, $\tau = (t - z/v_g)/\tau_p$ is the normalized retarded time for the pulse traveling at group velocity v_g , and p^{nl} is the suitably normalized nonlinear polarization. The presence of the operator $(1 + i\partial/\omega_0\tau_p\partial\tau)$ accounts for self-steepening effects¹⁴ and allows for modeling of the propagation of pulses with spectral widths comparable to the central frequency, ω_0 . The effects of both instantaneous (i.e., electronic) and non-instantaneous (i.e., nuclear) nonlinear refractive-index changes in the nonlinear polarization are included such that

$$p^{nl}(\zeta, \tau) = \frac{L_{ds}}{L_{nl}} \left[(1-f) |u(\zeta, \tau)|^2 + f \int_{-\infty}^{\tau} d\tau' R(\tau - \tau') |u(\zeta, \tau')|^2 \right] u(\zeta, \tau), \quad (2)$$

where $L_{nl} = (c/\omega_0 n_2 I_0)$ is the nonlinear length, $I_0 = n_0 c |A_0|^2 / 2\pi$ is the peak input intensity, $n_2 = 2 \times 10^{-16}$ cm²/W is the nonlinear refractive-index coefficient of fused-silica glass, f is the fraction of the Raman contribution to the nonlinear refractive index, and $R(\tau)$ is the Raman response function.^{15,16}

In the simulations described here, parameters are used that correspond to the case¹ of propagation of an initially 100-fs pulse FWHM ($\tau_p = 60$ fs) at 770 nm inside a fused-silica microstructured fiber with a core

size of $1.7 \mu\text{m}$ in diameter, that is, $L_{\text{ds}} = 500 \text{ cm}$, $\omega_0 \tau_p = 140$, $L_{\text{ds}}/L_{\text{ds}}^{(3)} = 0.5$, $L_{\text{ds}}/L_{\text{ds}}^{(4)} = -0.005$, and $f = 0.15$. For a peak power of 1 kW, $L_{\text{ds}}/L_{\text{nl}} = 500$. The qualitative nature of the results described here occurs over a broad range of parameters and does not depend sensitively on the precise values.

We first consider the case in which the central wavelength of the pulse is tuned slightly to the long-wavelength side of the zero group-velocity dispersion point (i.e., $\beta_2 < 0$). At low powers and short propagation distances, the pulse exhibits asymmetric spectral broadening as a result of TOD, stimulated Raman scattering, and self-steepening. At intermediate powers ($P = 1 \text{ kW}$) and sufficiently long propagation distances ($L/L_{\text{ds}} = 0.025$), a peaked feature appears in the spectrum at the blue edge [see Fig. 1(a)]. There is no corresponding peak to the red side of the spectrum, and thus the appearance of this feature cannot be attributed simply to four-wave mixing. The corresponding time-domain behavior is shown in Fig. 1(b). The interplay of TOD and self-phase modulation gives rise to an abrupt phase drop between the two peaks, as indicated by the sharply peaked frequency chirp (d ϕ /d τ , where ϕ is the instantaneous phase of the field envelope), and yields the observed blue spectral feature. For longer propagation distances ($L/L_{\text{ds}} = 0.04$) [see Fig. 1(c)] the pedestal on the short-wavelength side becomes more prominent, and, as shown in Fig. 1(d), the corresponding time-domain profile of the light exhibits a progressively more complicated substructure. Further increases in the input power (see Fig. 2) result in extension of the blue edge of the spectrum further to shorter wavelengths, which is in agreement with experimental observations¹⁷ and is a result of the corresponding increase in the steepness of the phase drop at the point of the initial temporal splitting.

At still higher powers the spectral envelope becomes relatively flat such that the central portion [see Fig. 3(a)] is no longer prominent. This envelope is similar in shape to the supercontinuum spectrum observed in experiments; the blue edge is sharp and extends nearly to the ultraviolet, whereas the red edge falls off more gradually and, in terms of frequency, extends far less than does the short-wavelength side. Although SRS and self-steepening are included in this model, it is found that in the limit where the group-velocity dispersion is small, the basic shape depends primarily on the amount of TOD and to a lesser extent the amount of fourth-order dispersion. The corresponding time-domain behavior becomes highly complex, with the initial pulse breaking up into numerous pulses, some of which are significantly shorter than the initial pulse.

Although at these powers changes in the input pulse energy do not significantly alter the spectral envelope, the simulations indicate that the fine substructure in the simulations is extremely sensitive to the initial pulse energy. For example, an increase of 0.1% in the pulse energy under the same conditions produces the spectrum in Fig. 3(b), with an envelope that is nearly identical to that in Fig. 3(a). However, close inspection of the two spectra [Fig. 3(c)] illustrates that

small changes in pulse energy dramatically alter the fine substructure. Since the typical fluctuations in a mode-locked solid-state laser are of the order of 0.1%, it is expected that this substructure will exhibit strong fluctuations. We believe that this substructure and these large fluctuations have not been observed in most of the experimental spectra either because of insufficient spectral resolution or as a result of the fact that the spectra are an average of many laser pulses. However, a recent experiment⁹ in which single-pulse

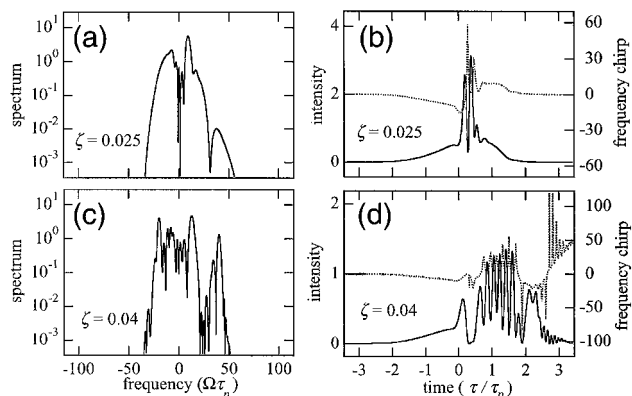


Fig. 1. (a), (c) Spectra and (b), (d) temporal profiles (solid curves) and frequency chirp (dotted curves) of the initially 100-fs ($\tau_p = 60 \text{ fs}$) pulse at two propagation distances ζ inside the fiber for the case in which the input power is 1 kW. In (a) and (c), full scale ($\Omega\tau_p = 100$) corresponds to $2.65 \times 10^{14} \text{ Hz}$.

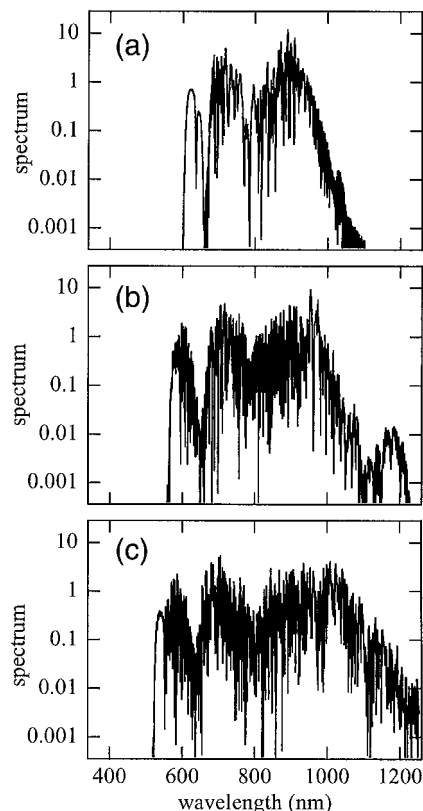


Fig. 2. Plots of the output spectrum of the transmitted pulse for increasing peak input power P : (a) $P = 2 \text{ kW}$, (b) $P = 4 \text{ kW}$, and (c) $P = 8 \text{ kW}$.

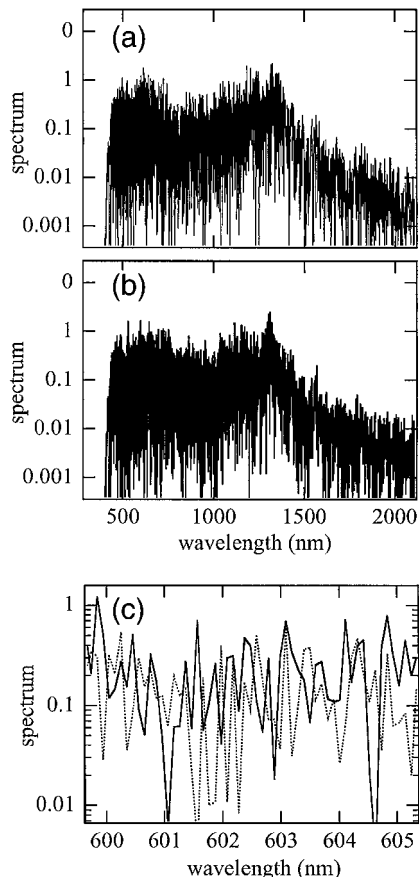


Fig. 3. (a) Output spectrum for an input peak power $P = 16$ kW and propagation distance $\zeta = 0.5$. (b) Same as (a) but with 0.1% higher peak power. (c) High-resolution window of the spectra in (a) (solid curve) and (b) (dotted curve).

spectra were obtained confirms the existence of this fine substructure and its sensitivity to input pulse energy. In certain cases this sensitivity to input fluctuations could impose limitations on the applicability of this fiber supercontinuum.

Since TOD primarily determines the dynamics that leads to the supercontinuum, manipulation of its magnitude and sign will play a crucial role in optimizing the shape and width of the spectrum for particular applications. For example, by changing the sign of the TOD (i.e., of β_3) but keeping all other parameters the same, one can substantially extend the red edge of the spectrum, whereas the extent of the blue edge is reduced. Generation of supercontinuum further into the infrared could thus be achieved by operation at the long-wavelength, second zero-GVD point¹⁸ of these fibers. We believe that suitable designs of microstructured fibers offer the possibility of further

increases in the total spectral bandwidth by reduction of the air-filling fraction of the microstructural fibers and thus decreased TOD and flattening of the dispersion profile.

I gratefully acknowledge discussions with S. Cundiff, S. Diddams, K. Moll, D. Ouzounov, J. Ranka, and R. Trebino. This work was supported through U.S. Army Research Office grant DAAD19-01-10341 and National Science Foundation grant PHY-9987990. A. Gaeta's e-mail address is a.gaeta@cornell.edu.

References

1. J. K. Ranka, R. S. Windeler, and A. J. Stentz, *Opt. Lett.* **25**, 25 (2000).
2. I. Hartl, X. D. Li, C. Chudoba, R. K. Ghanta, T. H. Ko, J. G. Fujimoto, J. K. Ranka, and R. S. Windeler, *Opt. Lett.* **26**, 608 (2001).
3. See, for example, D. J. Jones, S. A. Diddams, J. K. Ranka, A. Stentz, R. S. Windeler, J. L. Hall, and S. T. Cundiff, *Science* **288**, 635 (2000).
4. See also S. A. Diddams, D. J. Jones, J. Ye, S. T. Cundiff, J. L. Hall, J. K. Ranka, R. S. Windeler, R. Holzwarth, T. Udem, and T. Hänsch, *Phys. Rev. Lett.* **84**, 5102 (2000).
5. T. A. Birks, W. J. Wadsworth, and P. St. J. Russell, *Opt. Lett.* **25**, 1415 (2000).
6. G. P. Agrawal and M. J. Potasek, *Phys. Rev. A* **33**, 1765 (1986).
7. P. Beaud, W. Hodel, B. Zysset, and H. P. Weber, *IEEE J. Quantum Electron.* **QE-23**, 1938 (1987).
8. V. Yanofsky and F. W. Wise, *Opt. Lett.* **19**, 1547 (1994).
9. G. Boyer, *Opt. Lett.* **24**, 945 (1999).
10. X. Gu, L. Xu, M. Kimmel, E. Zeek, P. O'Shea, A. P. Shreenath, R. Trebino, and R. S. Windeler, "Frequency-resolved optical gating and single-shot spectral measurements reveal fine structure in microstructure-fiber continuum," *Opt. Lett.* (to be published).
11. P. V. Mamyshev and S. V. Chernikov, *Opt. Lett.* **15**, 1076 (1990).
12. T. Brabec and F. Krausz, *Phys. Rev. Lett.* **78**, 3283 (1997).
13. See, for example, G. P. Agrawal, *Nonlinear Fiber Optics*, 3rd. ed. (Academic, San Diego, Calif., 2001), Chap. 1.
14. G. Yang and Y. R. Shen, *Opt. Lett.* **9**, 510 (1984).
15. R. H. Stolen, J. P. Gordon, W. J. Tomilson, and H. A. Haus, *J. Opt. Soc. Am. B* **6**, 1159 (1989).
16. R. H. Stolen and W. J. Tomilson, *J. Opt. Soc. Am. B* **9**, 565 (1992).
17. J. K. Ranka, R. S. Windeler, and A. J. Stentz, in *Conference on Lasers and Electro-Optics*, 1999 OSA Technical Digest Series (Optical Society of America, Washington, D.C., 1999), postdeadline paper CD-8.
18. J. C. Knight, J. Arriga, T. A. Birks, A. Ortigasa-Blanch, W. J. Wadsworth, and P. St. J. Russell, *IEEE Photon. Technol. Lett.* **12**, 807 (2000).